

Electrochemistry of Spontaneously Adsorbed Monolayers. Effects of Solvent, Potential, and Temperature on Electron Transfer Dynamics

Robert J. Forster and Larry R. Faulkner*

Contribution from the Department of Chemistry, University of Illinois, 600 S. Mathews Avenue, Urbana, Illinois 61801

Received November 29, 1993*

Abstract: The heterogeneous electron transfer kinetics for spontaneously adsorbed monolayers of $[\text{Os}(\text{bpy})_2\text{Cl}(\text{pNp})]\text{-PF}_6$, where bpy is 2,2'-bipyridyl and pNp is 1,2-bis(4-pyridyl)ethane or 4,4'-trimethylenedipyridine, have been explored using short time scale potential step chronoamperometry. For the $\text{Os}^{2+}/^{3+}$ redox reaction, heterogeneous electron transfer is a rapid first-order process characterized by a single unimolecular rate constant (k/s^{-1}). Temperature-resolved measurements of k have typically been made over the temperature range -5 to $+40$ °C and have been used to determine the ideal electrochemical enthalpy, $\Delta\bar{H}_1^\ddagger$. The ability of the Butler–Volmer equation to accurately describe the potential dependence of the enthalpy and entropy of activation has been investigated. The electrical component of $\Delta\bar{H}_1^\ddagger$ is considerably less sensitive to potential than is predicted by the Butler–Volmer formulation. The influence of solvent on the kinetics and thermodynamics of electron transfer has been explored in acetonitrile, acetone, dimethylformamide, dichloroethane, tetrahydrofuran, and chloroform. For the p2p monolayers, the standard rate constants k° range from $7.4 \times 10^3 \text{ s}^{-1}$ in chloroform to $1.1 \times 10^5 \text{ s}^{-1}$ in acetonitrile, while for the p3p monolayers the k° values are 1.6×10^3 and $1.8 \times 10^4 \text{ s}^{-1}$, respectively. For both these monolayers, a linear correlation is observed between $\ln k^\circ$ in $\ln \tau_l$, where τ_l is the longitudinal relaxation rate of the solvent. The slope of the plot is negative and near unity, suggesting that electron transfer is strongly influenced by solvent reorganization dynamics. The ideal electrochemical activation enthalpy has been determined as a function of the solvent for the p3p monolayer. The reaction enthalpy $T\Delta S_{rc}^\circ$, which is the difference in the anodic and cathodic values of $\Delta\bar{H}_1^\ddagger$ at the formal potential, gives an entropy that is considerably less sensitive to the solvent than the ΔS_{rc}° values obtained from temperature-resolved measurements of the formal potential. The dependence of the corresponding free energy changes on solvent is discussed in relation to the Marcus theory. The electronic transmission coefficient κ_{el} describing the probability of electron transfer once the nuclear transition state has been reached is calculated from the preexponential factor. This analysis shows that κ_{el} is considerably less than unity, suggesting a nonadiabatic reaction, which is anticipated for long-range electron transfers. However, the observation that solvent dynamics influence the electron transfer kinetics, while there is weak spatial orbital overlap, is unexpected from current electron transfer models.

Introduction

The dependence of the heterogeneous rate constant k on potential and temperature has long been considered to be accurately described by the Butler–Volmer formulation of electrode kinetics.¹ This representation predicts an exponential dependence of k on the driving force (overpotential), while the temperature dependence arises from an electrochemical Arrhenius equation involving an exponent in $1/RT$, where R is the gas constant and T is the absolute temperature. However, recent investigations by Conway and co-workers² of mechanistically complex systems, such as the hydrogen evolution reaction, suggest that the predicted dependence of k on potential and temperature is rarely observed. These observations suggest that at least for reactions involving atom transfer, the Butler–Volmer equation may be inadequate. The situation regarding simple electron transfer reactions involving ionic reactants has been explored only for a limited variety of redox couples,³ in part because mass

transport limits the potential range over which the rates can be investigated. This mass transport limitation can be circumvented by immobilizing a monolayer of the redox active species directly onto the electrode surface.

In this paper, we report on the kinetics and thermodynamics of heterogeneous electron transfer at spontaneously adsorbed monolayers as a function of solvent and potential. The rate constants are measured for the $\text{Os}^{2+}/^{3+}$ redox reaction within monolayers of $[\text{Os}(\text{bpy})_2\text{Cl}(\text{pNp})]^+$, where bpy is 2,2'-dipyridyl and pNp is either 1,2-bis(4-pyridyl)ethane or 4,4'-trimethylenedipyridine. We denote the monolayers as p2p and p3p, respectively. For these monolayers, Tafel plots of $\ln k$ vs overpotential are nonlinear at large overpotentials,⁴ which is not predicted by the Butler–Volmer equation. However, the response is accurately modeled by the Marcus theory.⁵ Here, we have extended this experimental test of the Butler–Volmer equation by comparing the predicted potential dependence of the electrochemical enthalpy with that experimentally observed. In this way we can test the accuracy of the thermodynamic and kinetic predictions. These experiments represent a meaningful attempt to test the validity of existing formulations of electrode kinetics using an electron transfer reaction that shows nearly ideal electrochemical responses,

* Author to whom correspondence should be addressed.

• Abstract published in *Advance ACS Abstracts*, May 15, 1994.

(1) Bard, A. J.; Faulkner, L. R. *Electrochemical Methods: Fundamentals and Applications*; Wiley: New York, 1980.

(2) (a) Conway, B. E.; Wilkinson, D. P. *J. Chem. Soc., Faraday Trans. 1989*, 85, 2355. (b) Conway, B. E. *Modern Aspects of Electrochemistry*; Conway, B. E., White, R. E., Bockris, J. O'M., Eds.; Plenum Press: New York, 1985; Vol. 16, Chapter 2. (c) Conway, B. E.; Angerstein-Kozłowska, H.; Sattar, M. A.; Tilak, B. V. *J. Electrochem. Soc.* 1983, 130, 1825. (d) Conway, B. E.; MacKinnon, D. J.; Tilak, B. V. *Trans. Faraday Soc.* 1970, 66, 1203. (e) Conway, B. E.; Tessier, D. F.; Wilkinson, D. P. *J. Electrochem. Soc.* 1989, 136, 2486.

(3) (a) Weaver, M. J. *J. Phys. Chem.* 1979, 83, 1748. (b) Weaver, M. J. *J. Phys. Chem.* 1976, 80, 2645. (c) Yee, E. L.; Cave, R. J.; Guyer, K. L.; Tyma, P. D.; Weaver, M. J. *J. Am. Chem. Soc.* 1979, 101, 1131.

(4) Forster, R. J.; Faulkner, L. R. *J. Am. Chem. Soc.*, preceding paper in this issue.

(5) Marcus, R. A. *J. Chem. Phys.* 1965, 43, 679.

even at nanosecond time scales. We observe experimentally that the electrochemical enthalpy is much less sensitive to potential than anticipated. Our data suggest that this situation arises because the entropy of activation depends significantly on potential, a feature that is ignored in the Butler–Volmer formulation.

Beyond potential and temperature, another parameter that may influence the electrode kinetics is the electrochemical solvent. The influence of solvent static and dynamic properties on the rate of electron transfer in solution has been an area of active interest for some time.^{6–8} However, the presence of work terms, imaging effects, and the requirement of assuming a value for the precursor stability constant, often prevent a complete description of these solvent effects for solution species.⁹ In contrast, adsorbed monolayers reduce or completely remove these difficulties typically associated with diffusive systems. However, adsorbed monolayers often contain redox centers that are held remotely from the electrode surface. The separation in systems already reported is typically about 20–30 Å,^{10–13} which implies that only weak electronic coupling is expected to occur between the electrode and the redox center. Existing electron transfer theory suggests that the ensuing nonadiabatic reaction would be completely insensitive to solvent dynamics, depending instead on the extent of spatial orbital overlap.⁸ For this reason, dynamic solvent effects have not been considered for these two-dimensional systems. In contrast to previously studied monolayers, the electron transfer distances explored in this paper are approximately 9 and 10 Å for the p2p and p3p monolayers, respectively. Given that the distance of closest approach is of the order of 5 Å for a solution species,¹ one might suspect that these systems would exhibit a different behavior versus that reported elsewhere for monolayers with longer bridging ligands.

The present films have several properties that make them especially attractive for investigating the influence of solvent dynamics on the electrode kinetics. These include small inner-shell barriers, chemical and physical stability, and facile interfacial kinetics in a range of solvents. We have investigated the functional dependence of the electron transfer rate on the solvent's relaxation time and show that it is approximately proportional to τ_l^{-1} , where τ_l is the longitudinal relaxation time of the solvent. This suggests that the electron transfer process is sensitive to the solvent's ability to relax dynamically to accommodate the new charge placed on the redox center.^{6–8}

We have also investigated the solvent dependence of the electrochemical free energy of activation and have compared our experimental observations with those predicted by the Marcus dielectric continuum theory.^{5,14,15} The adiabaticity of the reaction has been analyzed by calculating the electronic transmission coefficient κ_{el} from the standard rate constants using the experimentally determined free energy change. This analysis indicates that the reaction is nonadiabatic, suggesting weak spatial orbital overlap between the redox center and the electrode. The observation of a strong solvent dynamic effect, together with a nonadiabatic transmission coefficient, is wholly unexpected on

the basis of existing electron transfer theory. For weakly coupled reactants, one would expect the interfacial kinetics to be dictated by the coupling strength and not to depend on the solvent dynamics. The overall results obtained are important in extending our understanding of thermal activation and solvent reorganization for interfacial processes.

Experimental Section

The experimental procedures described in the preceding paper were followed.⁴ During temperature-resolved measurements of the electrode kinetics, the reference electrode was isolated from the main compartment of the cell using a salt bridge as described in the preceding paper⁴ and held at constant temperature. The rate constants were measured at a fixed potential using chronoamperometry, as the temperature of the working electrode was systematically altered. The temperature range was typically –5 to +40 °C, which was selected for the following reasons. Cyclic voltammograms recorded at the beginning and the end of an 8-h period, during which time the monolayers are at a constant 40 °C, were indistinguishable. This invariant response suggests that the monolayers are physically and chemically stable at the upper temperature limit. For the surface-confined redox centers considered here, heterogeneous electron transfer is a thermally activated process, and immeasurably large rate constants were observed at temperatures higher than 40 °C in some solvents. The upper temperature limit was also dictated by the boiling point of some of the solvents used. The lower temperature limit was selected to avoid problems with slow double layer charging and iR drop effects. Rate constants were measured only when the cell time constants were at least five times shorter than the lifetime of the Faradaic reaction. At temperatures below –5 °C, this condition could not always be maintained.

Results and Discussion

Temperature and Potential Dependence of k . For electrode reactions that are limited only by the interfacial kinetics, the Butler–Volmer formulation predicts an exponential dependence of the heterogeneous electron transfer rate k on overpotential, $\eta \equiv (E - E^\circ)$, where E° is the formal potential, that is defined here as the potential at which the forward and backward rate constants are equal. The situation for a one electron reduction reaction is described by eq 1:

$$k = k^\circ \exp[-\alpha_c F \eta / RT] \quad (1)$$

where k° is the standard rate constant, α_c is the cathodic transfer coefficient, and F is Faraday's constant.

In the preceding paper, we considered the potential dependence of $\ln k$ on η ,⁴ and found nonlinear responses at large overpotentials. If α_c is regarded as a constant, this behavior is not predicted by eq 1 which is a linear function of overpotential. The dependence of k on temperature is also widely accepted as being embodied in the Butler–Volmer equation, and it is this feature that we explore here.

A precedent exists for supposing that the temperature dependence of electrode kinetics may not be accurately described by eq 1 at least for complex inner-sphere reactions. Other workers² have made temperature-resolved measurements of Tafel slopes and found that temperature-dependent values of α are commonplace for the hydrogen evolution reaction at various metal electrodes, as well as for anodic N_2 , Br_2 , and O_2 evolution.^{16,2d,17} In contrast to the expected behavior, the Tafel slope for oxygen evolution at Pt and Os electrodes¹⁷ is independent of temperature. These observations point to a serious deficiency in the accepted description of electrode kinetics.

However, these reactions are complicated since atom transfer is involved. What is needed are measurements on the temperature and potential dependencies of the electrode kinetics for simple ionic reactants with proper corrections for double-layer effects.

(16) Stout, H. P. *Trans. Faraday Soc.* 1945, 64.

(17) (a) Appleby, A. J. *J. Electrochem. Soc.* 1970, 117, 1158. (b) Appleby, A. J. *J. Electroanal. Chem.* 1970, 27, 325.

(6) Zhang, X.; Leddy, J.; Bard, A. J. *J. Am. Chem. Soc.* 1985, 107, 3719.

(7) Zhang, X.; Yang, H.; Bard, A. J. *J. Am. Chem. Soc.* 1987, 109, 1916.

(8) (a) Weaver, M. J. *Chem. Rev.* 1992, 92, 463. (b) Bagchi, G. *Annu. Rev. Phys. Chem.* 1989, 40, 115. (c) Sutin, N. *Acc. Chem. Res.* 1982, 15, 275.

(9) Newton, M. D.; Sutin, N. *Annu. Rev. Phys. Chem.* 1984, 35, 437.

(10) Finklea, H. O.; Hanshaw, D. D. *J. Am. Chem. Soc.* 1992, 114, 3173.

(11) Chidsey, C. E. D. *Science* 1991, 251, 919.

(12) Porter, M. D.; Bright, T. B.; Allara, D.; Chidsey, C. E. D. *J. Am. Chem. Soc.* 1987, 109, 3559.

(13) Chidsey, C. E. D.; Bertozzi, C. R.; Putvinski, T. M.; Mujsc, A. M. *J. Am. Chem. Soc.* 1990, 112, 4301.

(14) (a) Marcus, R. A. *J. Chem. Phys.* 1956, 24, 966. (b) Marcus, R. A. *Annu. Rev. Phys. Chem.* 1964, 15, 155. (c) Sumi, H.; Marcus, R. A. *J. Chem. Phys.* 1986, 84, 4894.

(15) (a) Marcus, R. A.; Sutin, N. *Biochim. Biophys. Acta* 1985, 811, 265. (b) Marcus, R. A. *Special Topics in Electrochemistry*; Rock, P. A., Ed.; Elsevier: New York, 1977; p 161.

They would allow the temperature dependence of the transfer coefficient for an elementary electron transfer reaction to be better understood. In this paper we report on the first extensive attempt to achieve this objective. To approach it, we have measured the potential dependence of the ideal electrochemical enthalpy $\Delta\bar{H}_{1c}^*$ for the simple $\text{Os}^{2+/3+}$ redox reaction within spontaneously adsorbed monolayers.

The heterogeneous electron transfer rate is considered to depend on a frequency factor and a Franck–Condon barrier, and can be expressed as⁸

$$k = A_{\text{et}} \exp(-\Delta\bar{G}^*/RT) \quad (2)$$

where A_{et} is the pre-exponential factor and $\Delta\bar{G}^*$ is the electrochemical free energy of activation. For an adsorbed monolayer, the pre-exponential factor A_{et} is taken as $\Gamma_n \kappa_{\text{el}} \nu_n$, where Γ_n is the nuclear tunneling factor, κ_{el} is the electronic transmission coefficient, and ν_n is the nuclear frequency factor.^{18,19} Since the experimental frequency factors are always less than $k_{\text{B}}T/h$ (k_{B} and h are the Boltzmann and Planck constants, respectively), the nuclear tunneling factor, Γ_n is unity.⁸ We assume that it is temperature independent.

As has been discussed previously,^{1,20} $\Delta\bar{G}^*$ contains both “chemical” and “electrical” contributions to the driving force. The Galvani potential difference across the metal/solution interface ϕ_{m} determines the electrical driving force, which is often defined for a reduction reaction as $\exp[\alpha_{\text{c}}F\phi_{\text{m}}/RT]$ under the Butler–Volmer formulation of electrode kinetics. Separating $\Delta\bar{G}^*$ into chemical enthalpic and entropic contributions, as well as the electrical driving force, gives^{3a,b}

$$k = A_{\text{et}} \exp[-\Delta H^*/RT] \exp[\Delta S^*/R] \exp[\alpha_{\text{c}}F\phi_{\text{m}}/RT] \quad (3)$$

Potential Dependence of $\Delta\bar{H}_{1c}^*$. As Weaver and co-workers have established,^{21,22} a constant Galvani potential difference ϕ_{m} across the metal/solution interface can be achieved by using a nonisothermal cell. The electrochemical activation enthalpy determined from an Arrhenius plot of $\ln k$ vs $1/T$, where ϕ_{m} is held constant, has been termed “ideal”^{3a,b} and we label it here as $\Delta\bar{H}_{1c}^*$.

$$\Delta\bar{H}_{1c}^* = -R \partial \ln k / \partial (1/T) |_{\phi_{\text{m}}} = \Delta H^* - \alpha_{\text{c}}F\phi_{\text{m}} \quad (4)$$

Figure 1 shows the temperature dependence of the chronoamperometric $i(t)$ vs t transients for a p3p monolayer, where the supporting electrolyte is 0.1 M TEAP in DMF and the overpotential is -0.108 V. This figure is representative of all the situations investigated and shows that we can time-resolve the double-layer charging and Faradaic current delays. The lifetime of the Faradaic reaction decreases with increasing temperature, as anticipated for a thermally activated process. The inset in Figure 1 illustrates the corresponding semilog plots, the Faradaic component of which is typically linear over 2 lifetimes. The linear response is consistent with first-order kinetics. The fact that a single slope is observed for each temperature suggests that heterogeneous electron transfer is characterized by one rate constant. In a typical set of experiments, we systematically vary the temperature over a range and then return to the initial temperature. The same slope $-k$ and intercept $\ln(kQ)$, where Q is the total charge passed in the redox transformation, are observed for initial and final transients. This consistency suggests that cycling the temperature does not change the monolayer

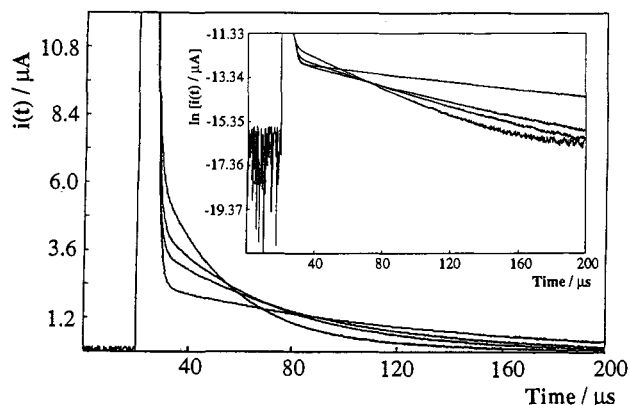


Figure 1. Current responses for a 25 μm platinum microelectrode modified with a p3p monolayer following potential steps where $\eta = -0.108$ V. At 40 μs the temperatures are, from top to bottom, 40, 25, 15, and -5 $^{\circ}\text{C}$, respectively. The supporting electrolyte is 0.1 M TEAP in DMF. The inset shows $\ln i(t)$ vs t plots for the current–time transients. At 120 μs the temperatures are, from top to bottom, -5 , 15, 25, and 40 $^{\circ}\text{C}$, respectively.

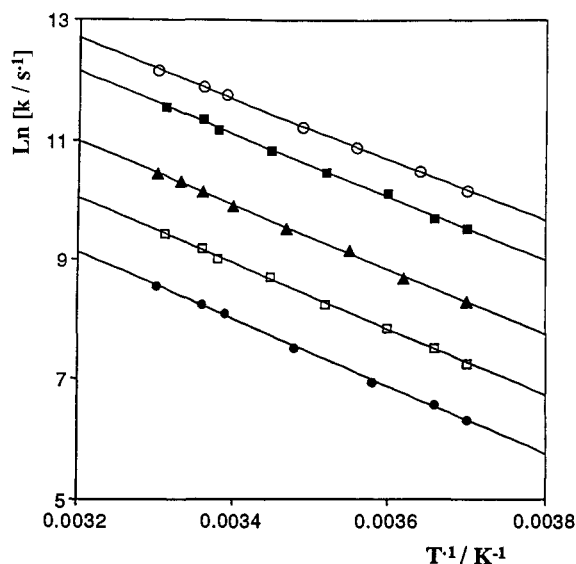


Figure 2. Arrhenius plots of $\ln k$ vs T for a p3p monolayer as a function of overpotential. The overpotentials are, from top to bottom, -0.250 , -0.211 , -0.150 , -0.097 , and -0.048 V, respectively. The electrolyte is 0.1 M TBAP in chloroform.

conformation or the quantity of material immobilized on the electrode surface. Figure 2 illustrates representative Arrhenius plots as a function of overpotential for a p3p monolayer, where the solvent is chloroform. Good linearity is observed over the temperature range investigated, and the slope $-\Delta\bar{H}_{1c}^*/R$ gives the ideal electrochemical enthalpy.

Figure 3 illustrates the experimentally observed dependence of the ideal electrochemical enthalpy on the electrical driving force for a p3p monolayer, where the solvent is CF. The expected slopes are $\alpha_{\text{a}}F\eta$ and $-\alpha_{\text{c}}F\eta$, for the oxidation and reduction processes, respectively. As described in the preceding paper,⁴ Tafel plots of $\ln k$ vs η are approximately linear for overpotentials less than about 0.2 V at room temperature, and we have calculated transfer coefficients, α_{a} and α_{c} , from the slopes. Table 1 shows that both α_{a} and α_{c} are close to the expected values of 0.5 for all solvents examined. Therefore, one expects absolute slopes of approximately $48 \text{ kJ mol}^{-1} \text{ V}^{-1}$ in Figure 3. However, the anodic and cathodic slopes, -12.8 and $13.8 \text{ kJ mol}^{-1} \text{ V}^{-1}$, respectively, are considerably smaller than expected. Table 1 also contains the apparent transfer coefficients obtained from the potential dependence of the ideal electrochemical enthalpy, as a function of the solvent. In all solvents examined markedly lower transfer

(18) Barr, S. W.; Guyer, K. L.; Li, T. T.-T.; Liu, H. Y.; Weaver, M. J. *J. Electrochem. Soc.* **1984**, *131*, 1626.

(19) Sutin, N.; Brunschwig, B. S. *ACS Symp. Ser.* **1982**, *198*, 105.

(20) Conway, B. E. *Theory and Principles of Electrode Processes*; Ronald Press: New York, 1965; Chapter 6.

(21) Li, T. T.; Guyer, K. L.; Barr, S. W.; Weaver, M. J. *J. Electroanal. Chem.* **1984**, *164*, 27.

(22) Yee, E. L.; Weaver, M. J. *Inorg. Chem.* **1980**, *19*, 1077.

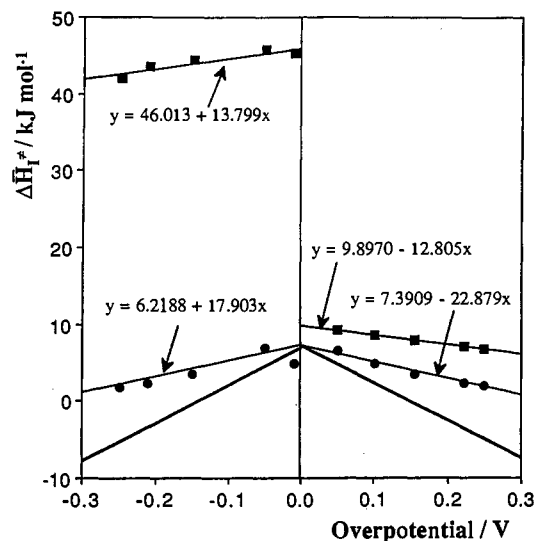


Figure 3. Dependence of the ideal electrochemical enthalpy, $\Delta\bar{H}_1^\ddagger$, on potential for a p3p monolayer where the electrolyte is 0.1 M TEAP in CF. Solid circles and squares represent the overlap integral model and the experimental data, respectively. The bold lines near the bottom represent the Butler-Volmer prediction.

Table 1. Transfer Coefficients for p3p Monolayers^a

solvent	α_a^b	α_c^b	α_a^c	α_c^c	$d\alpha_a/dT,^d \text{ K}^{-1}$	$d\alpha_c/dT,^d \text{ K}^{-1}$
AN	0.50	0.51	0.11	0.20	1e-3	1e-3
AC	0.48	0.53	0.18	0.30	1e-3	6e-4
DMF	0.50	0.49	0.18	0.30	1e-3	6e-4
THF	0.52	0.48	0.10	0.25	1e-3	7e-4
DCE	0.51	0.48	0.16	0.13	1e-3	1e-3
CF	0.48	0.53	0.14	0.14	1e-3	1e-3

^a Transfer coefficients are reproducible to within ± 0.05 between individual monolayers. ^b Determined from the slope of $\ln k$ vs η plots for $|\eta| < 200$ mV. ^c Determined from the potential dependence of the ideal electrochemical enthalpy, $\Delta\bar{H}_1^\ddagger$. See text for details. ^d Determined from the temperature dependence of the Tafel slope. See text for details.

coefficients are obtained from the potential dependence of the activation enthalpies compared to those obtained from the potential dependence of the rate constants. Importantly, this finding demonstrates that the electrical contribution to the observed ideal enthalpy is inconsistent with the classical Butler-Volmer formulation of electrode kinetics, in which α_c is assumed to be independent of potential and temperature.

Within the context of the Butler-Volmer framework, a possible reason why $\Delta\bar{H}_1^\ddagger$ does not depend on potential as expected is that the transfer coefficient increases linearly with increasing temperature. Since the magnitude of the electrical component is $\exp[\alpha F\phi_m/RT]$, the ideal enthalpy would then be less dependent on temperature than expected. We have explored this possibility by experimentally determining α_a and α_c as a function of the temperature in a range of solvents. Figure 4 shows the temperature dependence of Tafel plots of $\ln k$ vs η for Os^{2+} oxidation within p3p monolayers, where the solvent is DMF. The slopes of these plots are $\alpha_a F/RT$ thus giving α_a as a function of temperature. The temperature derivatives $d\alpha/dT$ are included in Table 1 as a function of the solvent. The data are close to the limit of our experimental precision, and they indicate that α_a and α_c are at best very weakly temperature dependent.

Nagy and co-workers²³ have considered the temperature dependence of the transfer coefficient for the ferrous-ferric system, which is known to be a simple electron transfer reaction. By measuring the heterogeneous electron transfer reaction rate over the temperature range from 25 to 275 °C, they were able to show that the transfer coefficient is temperature independent. This

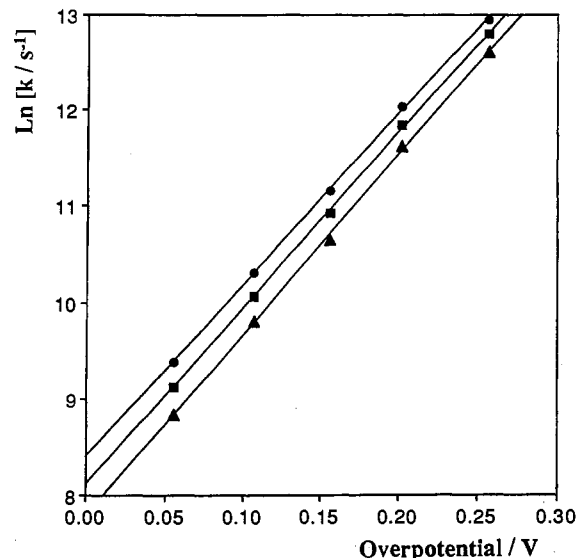


Figure 4. Tafel plots of $\ln k$ vs η as a function of temperature for a p3p monolayer. The electrolyte is 0.1 M TEAP in DMF. Temperatures are, from top to bottom, 40, 20, and 0 °C.

observation is consistent with the classical Butler-Volmer approach, and the authors suggest that temperature-dependent transfer coefficients are likely to arise from elementary steps other than simple charge transfer. Therefore, our observation that the transfer coefficients for the osmium monolayers discussed here are at best very weakly temperature dependent is consistent with our assertion that we are probing the elementary electron transfer event in a simple outer-sphere electron transfer. What is also evident from the temperature derivatives of the transfer coefficients (Table 1) is that they are much too small to explain the relative insensitivity of $\Delta\bar{H}_1^\ddagger$ to changes in η .

Since the chemical free energy component of the electrochemical enthalpy cannot depend on potential, our observations together suggest that the entropy of activation in eq 3 is potential dependent. The nuclear tunneling factor, frequency factor, and electronic transmission coefficient are likely to be approximately independent of the temperature and potential. Therefore, one can in principle investigate the potential dependence of ΔS^\ddagger by plotting the intercept of the Arrhenius plots $A_{et} \exp(\Delta S^\ddagger)$ as a function of potential. Figure 5 shows the dependence of $\ln [A_{et} \exp(\Delta S^\ddagger)]$ on η , where the solvent is DMF. This figure clearly shows that the entropy of activation depends markedly on the potential.

In the preceding paper,⁴ we successfully modeled the nonlinear Tafel plots using an overlap integral approach. In this model, the potential dependence of $\ln k$ for both branches and both monolayers was essentially reproduced using the Marcus solvent reorganization energy and an adjustable pre-factor, if we held the tunneling parameter β constant at the value obtained at E° . We have calculated the potential dependence of $\Delta\bar{H}_1^\ddagger$ using this model and the results are illustrated in Figure 3. Importantly, this approach predicts that $\Delta\bar{H}_1^\ddagger$ will be less sensitive to changes in potential than is predicted by the Butler-Volmer formulation. We have also calculated the potential dependence of the pre-exponential factor using this overlap integral approach, and the theoretical results are compared with the experimental data in Figure 5. Importantly, this model predicts both the sign and approximate magnitude of the slope for a plot of $\ln [A_{et} \exp(\Delta S^\ddagger)]$ versus η .

Our conclusion, on the basis of all these observations, is that the Butler-Volmer approach is not useful for understanding activation parameters of electrode kinetics, at least not in these systems.

Solvent Effects on the Interfacial Kinetics. Considerable experimental and theoretical research effort has been devoted to

(23) Curtiss, L. A.; Halley, J. W.; Hautman, J.; Hung, N. C.; Nagy, Z.; Rhee, Y. J.; Yonco, R. M. *J. Electrochem. Soc.* **1991**, *138*, 2032.

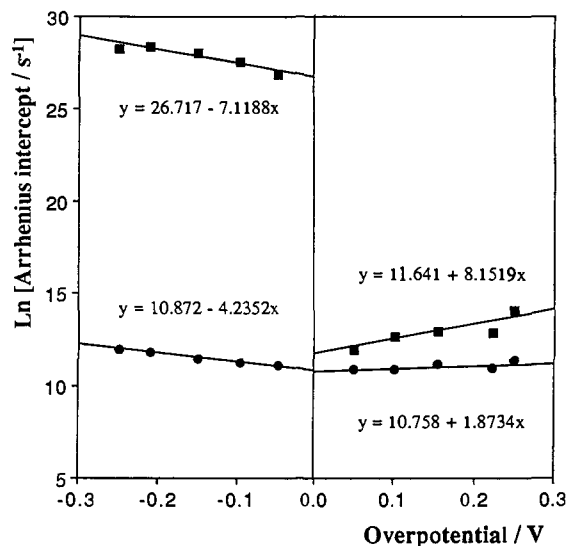


Figure 5. Dependence of the logarithm of the Arrhenius intercept on overpotential, for a p3p monolayer. The electrolyte is 0.1 M TEAP in DMF. Solid circles and squares represent the overlap integral model and the experimental data, respectively.

the effect of solvent dielectric relaxation on both heterogeneous and homogeneous electron transfer kinetics.²⁴⁻²⁹ The electrochemical solvent can influence the electron transfer rate through either its static or dynamic properties because of the noninstantaneous rearrangement of the solvent dipole that must precede electron transfer. Static properties, such as dielectric constants, can alter the activation barrier for electron transfer, while a dynamic property, such as a relaxation time, can affect the relative motion of the reactant along the reaction coordinate near the transition state. For simplicity, we call these effects "static" and "dynamic", respectively, in the remainder of this paper.

To examine the effect of solvent reorganization on the electron transfer kinetics, we have determined the standard heterogeneous rate constant as a function of τ_l , the longitudinal dielectric relaxation time of the solvent.³⁰ A single unimolecular rate constant characterized heterogeneous electron transfer in all solvent systems examined, suggesting that order is preserved within the monolayer in organic media. The ability of the adsorbed monolayer to maintain a coherent structure in organic solvents is important, and it is a key feature in the successful investigation of the solvent-dependent reaction kinetics. For the p2p monolayers, the standard electron transfer rate apparently depends strongly on the solvent and varies from $7.4 \times 10^3 \text{ s}^{-1}$ in chloroform to $1.1 \times 10^5 \text{ s}^{-1}$ in acetonitrile. Table 2 gives k° as a function of solvent for both the p2p and p3p monolayers. Figure 6 illustrates the dependence of $\ln k^\circ$ on $\ln \tau_l$ for both p2p and p3p monolayers. This plot represents only a very rough guide to the role of overdamped solvent dynamics in the electron transfer process, since it neglects any solvent dependence of the activation barrier. We consider this effect later. We have tested for correlations between our experimental rate constants and other solvent properties including dielectric character, viscosity, and electrical conductance. The Pekar factor describes the dielectric character of the solvent and is equal to $(\epsilon_{op}^{-1} - \epsilon_s^{-1})$, where ϵ_{op} and ϵ_s are

(24) (a) Nielson, R. M.; McManis, G. E.; Safford, L. K.; Weaver, M. J. *J. Phys. Chem.* **1989**, *93*, 2152. (b) Nielson, R. M.; McManis, G. E.; Weaver, M. J. *J. Phys. Chem.* **1989**, *93*, 4703.

(25) (a) Weaver, M. J.; Gennett, T. *Chem. Phys. Lett.* **1985**, *113*, 213. (b) Gennett, T.; Milner, D. F.; Weaver, M. J. *J. Phys. Chem.* **1985**, *89*, 2787. (c) McManis, G. E.; Golovin, M. N.; Weaver, M. J. *J. Phys. Chem.* **1986**, *90*, 6563.

(26) Maroncelli, M.; MacInnis, J.; Fleming, G. R. *Science* **1989**, *243*, 1674.

(27) Barbara, P. F.; Walker, G. C.; Smith, T. P. *Science* **1992**, *256*, 975.

(28) Guarr, T.; McLendon, G. *Coord. Chem. Rev.* **1985**, *68*, 1.

(29) Barbara, P. F.; Jarzaba, W. *Adv. Photochem.* **1990**, *15*, 1.

(30) Baranski, A. S.; Winkler, K.; Fawcett, W. R. *J. Electroanal. Chem.* **1991**, *313*, 367.

Table 2. Solvent Parameters and Heterogeneous Electron Transfer Kinetics^a

solvent	τ_l , ^b ps	Pekar factor ^c	$10^{-4}k^\circ$, s ⁻¹	
			p2p	p3p
AN	0.2	0.529	11.02(0.30)	1.80(0.08)
AC	0.3	0.495	6.43(0.15)	1.33(0.04)
DMF	1.1	0.463	1.77(0.05)	0.35(0.01)
THF	1.6	0.388	1.03(0.03)	0.21(0.01)
DCE	1.7	0.384	0.91(0.03)	0.20(0.02)
CF	2.4	0.276	0.74(0.04)	0.16(0.01)

^a Inter-monolayer standard deviations ($r \geq 3$) are in parentheses.

^b Longitudinal solvent relaxation time taken from ref 29 and sources therein. ^c Defined as $(\epsilon_{op}^{-1} - \epsilon_s^{-1})$.

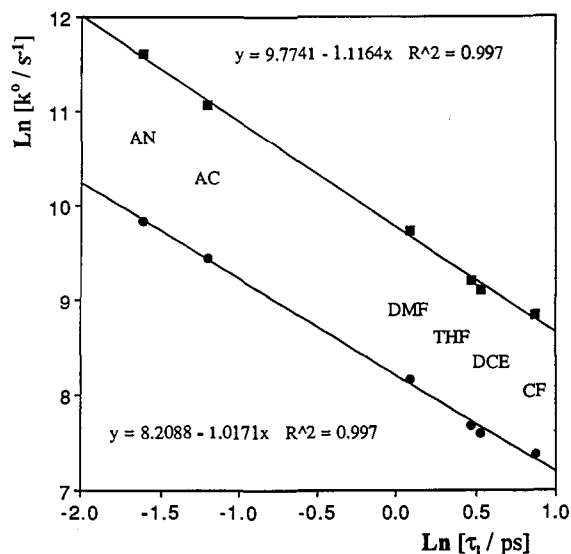


Figure 6. Dependence of the standard rate constants for p2p (top) and p3p (bottom) monolayers on the longitudinal relaxation time for the solvent (AN = acetonitrile, AC = acetone, DMF = dimethylformamide, THF = tetrahydrofuran, DCE = 1,2-dichloroethane, and CF = chloroform).

the optical and static dielectric constants, respectively. The logarithm of the heterogeneous rate constant correlates loosely with the Pekar factor ($R^2 \approx 0.85$). However, this is to be expected since the Pekar factor and τ_l are only pseudoindependent variables. We are currently probing the heterogeneous electron transfer rates in other solvents such as hexamethylphosphoramide, nitromethane, and dichloromethane to further investigate this correlation. The heterogeneous rate constants do not correlate with the electrical conductance of the solvent for either monolayer, suggesting that resistive effects are not contributing to the correlation observed in Figure 6. Furthermore, k° does not correlate with the solvent viscosity, which is consistent with our assertion that we are measuring the kinetics of the elementary transfer event, without mass transport, which would be sensitive to the solvent's viscosity.^{6,7}

Figure 6 shows a strong linear correlation with a near unity negative slope, suggesting a strong influence on the electron transfer rate from solvent relaxation dynamics,³⁰⁻³² despite the different electron transfer distances involved. To our best knowledge, this observation has not been previously reported for a spontaneously adsorbed monolayer. Chidsey's work with ferrocenethiol monolayers¹¹ suggests that the extent of electronic coupling between the metallic states of the electrode, and the redox center orbitals, controls the electron transfer rate. Under those circumstances, theory suggests that a correlation like that in Figure 6 would not be found, but the solvent dependence of

(31) Fawcett, W. R.; Foss, C. A. *J. Electroanal. Chem.* **1989**, *270*, 103.

(32) Weaver, M. J.; Phelps, D. K.; Nielson, R. M.; Golovin, M. N.; McManis, G. E. *J. Phys. Chem.* **1990**, *94*, 2949.

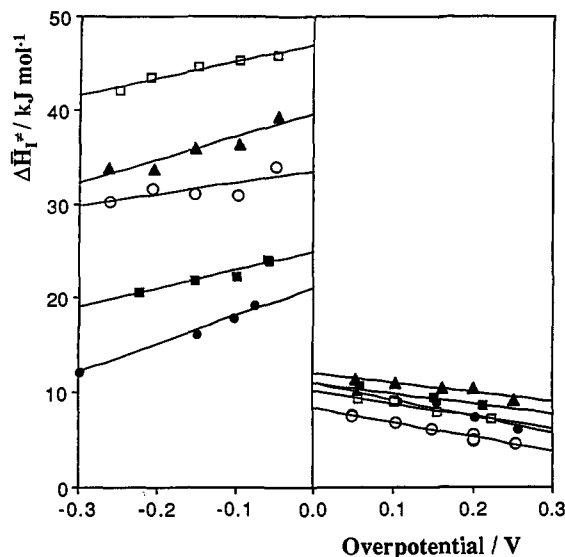


Figure 7. Dependence of the ideal electrochemical enthalpy ($\Delta\bar{H}_1^\ddagger$) on potential for p3p monolayers. Solvents, from top to bottom on the left-hand side, are CF, THF, DCE, AN, and DMF, respectively. Symbols on the right hand side correspond to those on the left.

Table 3. Reaction Entropies for p2p and p3p Monolayers^a

solvent	$\Delta S_{rc}^\circ(\text{Born}),^b$ J mol ⁻¹ K ⁻¹	$\Delta S_{rc}^\circ(\text{CV}),$ J mol ⁻¹ K ⁻¹		$\Delta S_{rc}^\circ(\text{CA}),^d$ J mol ⁻¹ K ⁻¹
		p2p ^c	p3p ^c	p3p ^c
AN	53	62(3)	65(4)	47(2)
AC	105	108(7)	88(4)	53(4)
DMF	62	79(5)	48(2)	34(2)
THF	240	237(8)	186(8)	95(6)
DCE	224	248(7)	152(8)	85(6)
CF	341	283(3)	252(12)	123(7)

^a Inter-monolayer standard deviations ($n \geq 3$) are in parentheses.

^b Calculated as described in ref 4 using the Born dielectric continuum model. ^c Determined from the temperature dependence of E° using a nonisothermal cell. See text for details. ^d Determined from the difference in the anodic and cathodic ideal electrochemical enthalpies obtained at E° . See text for details.

the electron transfer rate was not investigated experimentally in his work. It is interesting to note that a linear relationship exists between $\ln k^\circ$ and $\ln \tau_1$ despite the different degrees of ion pairing in these solvents.⁴ This is particularly important point and suggests that electron transfer proceeds independently of ion pairing.

Solvent Dependence of Activation Energies. We have determined the ideal electrochemical enthalpy $\Delta\bar{H}_1^\ddagger$ for p3p monolayers as a function of potential in the above solvents, and Figure 7 shows the results. We have already considered the potential dependence of these data, so we focus here on the significance of their absolute magnitudes and solvent dependencies. It is immediately apparent in Figure 7 that the $\Delta\bar{H}_1^\ddagger$ values obtained at E° are not equal for the oxidation and reduction reactions. The difference in intercepts is the reaction enthalpy ΔH_{rc}° , and since the free energy of activation is zero at the formal potential, it is equal to $T\Delta S_{rc}^\circ(\text{CA})$.³³ The reaction entropy $\Delta S_{rc}^\circ(\text{CA})$ quantifies the difference in order between the reduced and oxidized forms of the redox couple at short times.³⁴ In the preceding paper,⁴ we reported ΔS_{rc}° values obtained from the temperature dependence of the formal potential as measured using cyclic voltammetry, and we label it here as $\Delta S_{rc}^\circ(\text{CV})$. These two independent approaches provide an important opportunity for probing how rapidly equilibrium is established with respect to ion pairing and solvent ordering. Table 3 gives the solvent dependencies of $\Delta S_{rc}^\circ(\text{CA})$ and $\Delta S_{rc}^\circ(\text{CV})$ and shows that the

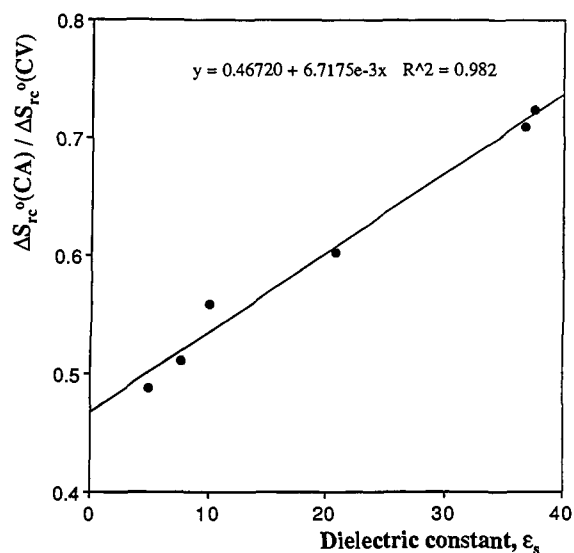


Figure 8. Dependence of the ratio $\Delta S_{rc}^\circ(\text{CA})/\Delta S_{rc}^\circ(\text{CV})$ for the p3p system on the static dielectric constant of the solvent.

chronoamperometric value is always smaller than that obtained using cyclic voltammetry. The relatively smaller $\Delta S_{rc}^\circ(\text{CA})$ values indicate that local ordering is less dependent on the oxidation state of the monolayer for the high-speed measurements. A possible explanation is that equilibrium ion pairing is established only on a relatively long time scale. Since ion pairing depends markedly on the dielectric constant of the solvent,⁴ one might expect the ratio of $\Delta S_{rc}^\circ(\text{CA})$ to $\Delta S_{rc}^\circ(\text{CV})$ to depend on the solvent. Figure 8 shows that this ratio tends toward unity only in high dielectric media, which is consistent with our previous conclusion that ion pairing was relatively less important in these solvents. It appears that because of the short time scales, the state immediately following a potential step is not at equilibrium with respect to ion pairing. This effect is likely to be especially important for oxidative potential steps, where movement of charge-compensating counterions is required to form an ion-paired monolayer.

In principle, it is possible to use the enthalpies and entropies discussed above to calculate free energies of activation. Comparing these values with the predictions of Marcus theory can give an insight into the importance of solvent reorganization in determining the activation barrier to electron transfer. The free energy of activation at the formal potential can be calculated using the ideal electrochemical enthalpies extrapolated to E° and $\Delta S_{rc}^\circ(\text{CV})$. For example, the cathodic free energy of activation $\Delta\bar{G}_c^\ddagger$ is given by

$$\Delta\bar{G}_c^\ddagger = \Delta\bar{H}_{1,c}^\ddagger - T\alpha_c\Delta S_{rc}^\circ(\text{CV}) - T\Delta S_{\text{int}}^\ddagger \quad (5)$$

where $\Delta S_{\text{int}}^\ddagger$ is the intrinsic reaction entropy, which is the difference between the two entropy changes from reactant to transition state and from transition state to product. In the following calculations, we first assume that the entropy of the transition state is midway between the entropies of the reactant and product, in which case $\Delta S_{\text{int}}^\ddagger$ is zero. Table 4 contains the solvent dependence of the cathodic and anodic free energies of activation for the p3p monolayers, together with the cathodic free energies of activation for the p3p systems. It is important to point out that the entropic contribution to the free energy of activation is significant, particularly in low dielectric solvents. For example, for the p3p monolayers in chloroform, $\Delta S_{rc}^\circ(\text{CV})$ is 252 J mol⁻¹ K⁻¹, thus $\alpha_c T\Delta S_{rc}^\circ(\text{CV})$ is 37.5 kJ mol⁻¹, a figure comparable to the cathodic ideal activation enthalpy of 46.8 kJ mol⁻¹.

As discussed earlier, Figure 6 suggests that dynamic solvent properties, such as the longitudinal relaxation rate, strongly

(33) Hupp, J. T.; Weaver, M. J. *J. Phys. Chem.* **1984**, *88*, 6128.

(34) Hupp, J. T.; Weaver, M. J. *J. Phys. Chem.* **1984**, *88*, 1860.

Table 4. Effect of Solvent on Activation Parameters^a

solvent	ΔG_{OS}^* , ^b kJ mol ⁻¹	$\Delta \bar{G}_c^*$, ^c kJ mol ⁻¹		$\Delta \bar{G}_a^*$, ^d kJ mol ⁻¹
		p2p	p3p	p3p
AN	12.3	11.4(0.4)	15.2(1.7)	20.6(1.6)
AC	11.5	10.3(0.3)	14.2(1.3)	24.7(1.8)
DMF	10.7	9.9(0.3)	13.9(1.4)	18.1(1.5)
THF	9.0	8.1(0.2)	11.9(1.1)	39.7(4.1)
DCE	8.8	8.4(0.2)	10.8(1.3)	31.0(3.2)
CF	6.4	5.6(0.2)	9.4(1.6)	47.7(4.4)

^a Inter-monolayer standard deviations ($n \geq 3$) are given in parentheses.

^b The Marcus outer-sphere reorganization energy calculated using eq 6.

^c Free energy of activation determined from the cathodic ideal electrochemical enthalpies at E^0 for using the values of ΔS_{rc}^0 (CV) given in Table 3. See text for details. ^d Free energy of activation determined from the anodic ideal electrochemical enthalpies at E^0 for using the values of ΔS_{rc}^0 (CV) given in Table 3. See text for details.

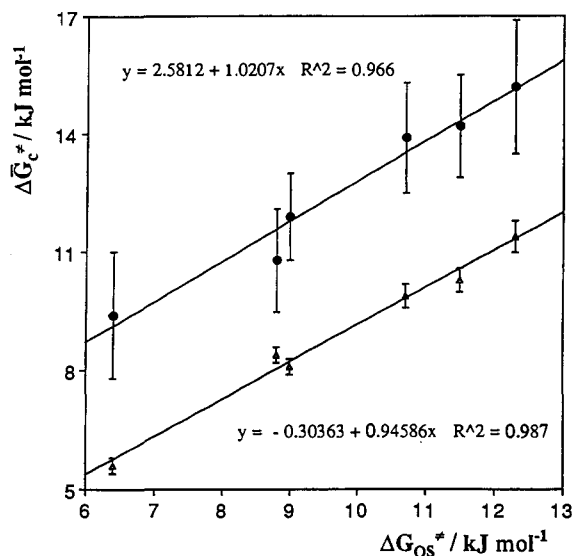


Figure 9. Correlation between $\Delta \bar{G}_c^*$ and $\Delta \bar{G}_{OS}^*$, the Marcus outer-sphere reorganization energy (eq 6). The p3p monolayer data are on the top, while the p2p monolayer data are on the bottom.

influence the heterogeneous electron transfer rate. If solvent dynamics control the heterogeneous electron transfer kinetics, then one might expect the activation barrier to be dictated by solvent dipole reorganization, which can be calculated from the Marcus theory,³⁵

$$\Delta G_{OS}^* = r^{-1}(\Delta e^2/8)(\epsilon_{op}^{-1} - \epsilon_s^{-1}) \quad (6)$$

where e is the electronic charge, r is the radius of the osmium complex (7.5 Å),³⁶ and ϵ_{op} and ϵ_s are the optical and static dielectric constants, respectively. In calculating ΔG_{OS}^* , we have neglected stabilizing imaging reactions.⁴ Table 4 contains the values as a function of the solvent.

Figure 9 shows that $\Delta \bar{G}_c^*$ correlates strongly with ΔG_{OS}^* , and a near unity slope is obtained for both monolayers. This apparently direct correlation suggests that outer-sphere reorganization determines the activation barrier for monolayer reduction. In the Marcus theory, the free energy of activation is equal to $\lambda/4$, where λ is the solvent reorganization energy. Therefore, an important test of self-consistency is to compare the values of $\Delta \bar{G}_c^*$ with the solvent reorganization energies. In the preceding paper, we reported λ values obtained by fitting the nonlinear Tafel plots using an electron tunneling model in which the tunneling parameter β was assumed to be independent of potential.

(35) Marcus, R. A. *Annu. Rev. Phys. Chem.* **1964**, *15*, 155.

(36) (a) Goodwin, H. A.; Kepert, D. L.; Patrick, J. M.; Skelton, B. W.; White, A. H. *Aust. J. Chem.* **1984**, *37*, 1817. (b) Ferguson, J. E.; Love, J. L.; Robinson, W. T. *Inorg. Chem.* **1972**, *11*, 1662. (c) Rillema, D. P.; Jones, D. S.; Levy, H. A. *J. Chem. Soc., Chem. Commun.* **1979**, 849.

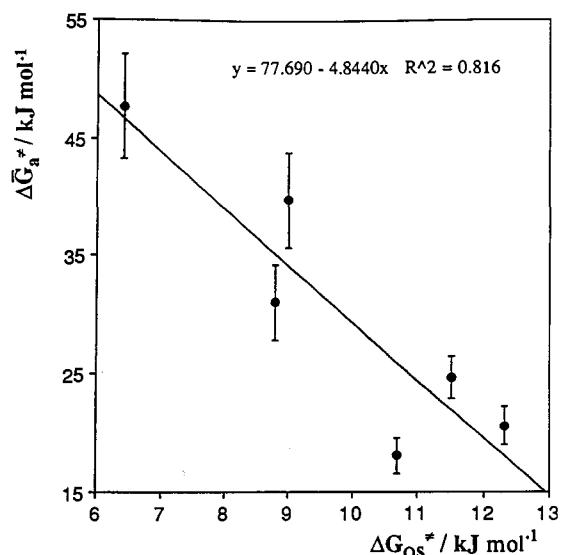


Figure 10. Correlation between $\Delta \bar{G}_a^*$ and ΔG_{OS}^* , the Marcus outer-sphere reorganization energy (eq 6) for p3p monolayers.

This approach gives the solvent reorganization energy without making temperature resolved measurements of k . In THF, DCE, and CF, where we can determine k over a sufficiently wide potential range to accurately model the observed responses, λ was determined to be 57, 50, and 38 kJ mol⁻¹, respectively. In all three cases, $\Delta \bar{G}_c^*$ and $\lambda/4$ agree to within 20%. In the other solvents, relatively more rapid heterogeneous electron transfer kinetics restricts the range of potentials over which k can be accurately measured. The Tafel plots are not highly curved within this working range, and accurate λ values cannot be obtained. However, these Tafel plots provide a lower limit for λ that is consistent with the $\Delta \bar{G}_c^*$ values reported here.

A sharply contrasting picture arises in Figure 10, which shows that the anodic free energies of activation $\Delta \bar{G}_a^*$ decrease with increasing ΔG_{OS}^* . Moreover, the estimates of $\Delta \bar{G}_a^*$ seem unreasonably large. For example, the free energy of activation observed in chloroform would yield a solvent reorganization energy of approximately 190 kJ mol⁻¹, which greatly exceeds the highest λ of 37 kJ mol⁻¹ that accurately fits the experimental Tafel plots.

That $\Delta \bar{G}_c^*$ apparently correlates positively with ΔG_{OS}^* , while $\Delta \bar{G}_a^*$ does not, could be an artifact of our use of the Butler-Volmer formalism to apportion the enthalpic and entropic contributions to the free energy of activation. In the preceding discussions, we have shown that this approach is not useful in describing the potential dependence of the rate constant, the electrochemical enthalpy of activation, or the entropy of activation. It is possible, therefore, that our apparently opposing correlations of $\Delta \bar{G}_c^*$ and $\Delta \bar{G}_a^*$ with ΔG_{OS}^* are simply another demonstration that this classical theory is not beneficial to understanding activation parameters within these systems.

On the other hand, the complicated oxidative behavior may arise because the monolayer fails to reach equilibrium with respect to ion pairing on the microsecond time scale. The kinetics of ion-pair dissociation could be sufficiently fast that the state reached immediately after monolayer reduction has nearly equilibrium ion pairing, whereas the requirement of ion-pair reassembly results in a state that is far from equilibrium for an oxidizing step. Such differences in the ion-pairing conditions of the states that immediately follow electron transfer would cause the entropy of activation to be intrinsically unequal in the two directions. In these circumstances, the equilibrium entropy given by ΔS_{rc}^0 (CV) would reflect entropy contributions arising from solvent ordering (fast) and assembly of an ion-paired monolayer (slow). If equilibrium ion pairing is not achieved for an oxidative step on the microsecond time scale, then ΔS_{rc}^0 (CV) would overestimate the relevant entropy. Calculating $\Delta \bar{G}_a^*$ using ΔS_{rc}^0 (CV) would

Table 5. Effect of Solvent on Pre-exponential and Related Parameters^a

solvent	$10^{-6}A_{et}, b\ s^{-1}$		$\nu_n, c\ ps^{-1}$	
	p2p	p3p	p2p	p3p
AN	29.0(8.1)	8.6(2.2)	3.03	3.40
AC	10.9(2.4)	3.9(0.1)	1.92	2.25
DMF	2.5(0.2)	1.0(0.2)	0.51	0.67
THF	0.71(0.12)	0.26(0.06)	0.32	0.38
DCE	0.70(0.14)	0.40(0.07)	0.57	0.35
CF	0.20(0.05)	0.07(0.01)	0.17	0.29

^a Inter-monolayer standard deviations ($n \geq 3$) are given in parentheses.

^b Pre-exponential factor, extracted from the rate constant using the $\Delta\bar{G}_c^*$ values given in columns 3 and 4 of Table 4. ^c Nuclear frequency factor calculated according to eq 7. See text for details.

give free energies of activation that are too large, and that do not correlate with ΔG_{OS}^* . Preliminary data on the electrolyte concentration dependence of $\Delta\bar{H}_{1,a}^*$ and $\Delta\bar{H}_{1,c}^*$ obtained at E^0 in DMF may support this interpretation. These data show that while the same cathodic activation enthalpies are obtained in 0.1 and 1.0 M solutions, $\Delta\bar{H}_{1,a}^*$ is uniformly smaller at all potentials where the supporting electrolyte concentration is 1.0 M.

Ion-pairing artifacts in intramolecular electron transfer reactions have been investigated by Hupp and co-workers using optical intervalence charge-transfer absorption measurements.³⁷ These investigations demonstrate that depending on whether electron transfer occurs sequentially or synchronously with ion translation, the extra energy associated with ion pairing can be viewed as either an unfavorable thermodynamic driving force or an additional component of the total reorganization energy. For our monolayers, the modest intercepts observed in Figure 9 for both the p2p ($-0.3\ kJ\ mol^{-1}$) and p3p ($+2.6\ kJ\ mol^{-1}$) monolayers suggest that the inner-sphere reorganization energy is small, which agrees with the facile interfacial kinetics observed. The absence of a significant inner-sphere reorganization energy suggests that ion pairing is not involved in the reduction process, and that the reported cathodic rate constants reflect the kinetics of the elementary electron transfer event. Therefore, we suggest that the different activation parameters for oxidation and reduction processes arise from a loss in the symmetry of the electron transfer process caused by the requirement of assembling an ion-paired monolayer in the oxidized state. The effect of counterion pairing is to render the initial and final states electrostatically, and hence energetically, inequivalent making the otherwise symmetrical electron transfer process asymmetric.

Pre-exponential Factor. The near unity negative slope observed in Figure 6 suggests that solvent dynamics strongly influence the electrode kinetics. However, this plot represents only a qualitative test since the solvent modulates both the activation barrier and the prefactor A_{et} . This complication can be avoided by investigating the dependence of A_{et} on the longitudinal relaxation rate of the solvent, τ_l .⁸ Given the free energy of activation, one can use eq 2 to determine A_{et} ($\equiv \kappa_{el}\nu_n$) without a convoluted entropy term. As discussed above, only the $\Delta\bar{G}_c^*$ correlates positively with ΔG_{OS}^* . Therefore, we have calculated A_{et} using only $\Delta\bar{G}_c^*$, and Table 5 summarizes data for both p2p and p3p monolayers as a function of the solvent. Figure 11 illustrates plots of $\ln A_{et}$ vs $\ln \tau_l^{-1}$. When Figures 6 and 11 are compared, it is apparent that correcting for the solvent dependence of the activation barrier (Figure 11) results in a weaker correlation with the longitudinal relaxation rate of the solvent. Furthermore, the slopes in Figure 11 exceed the value of unity expected for the situation where dynamic solvent properties (τ_l^{-1}), rather than static solvent properties (Pekar factor), dominate the prefactor.⁸

An adiabatic reaction involves considerable donor-acceptor coupling, so that the system remains on a single reaction

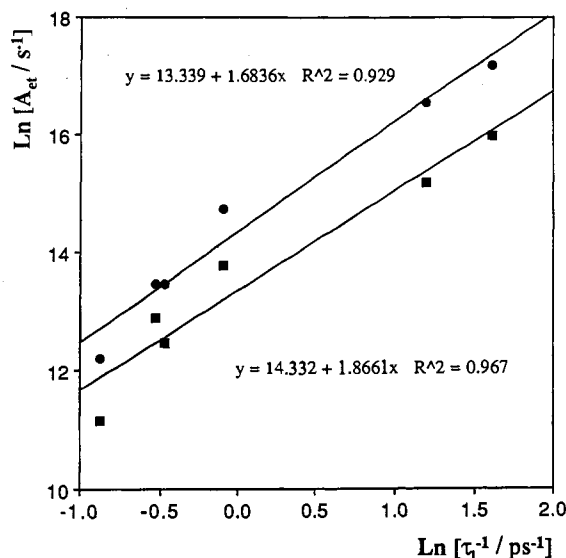


Figure 11. Dependence of the experimental pre-exponential factor A_{et} on the inverse longitudinal relaxation rate of the solvent. The p2p monolayer data are on the top, while the p3p monolayer data are on the bottom.

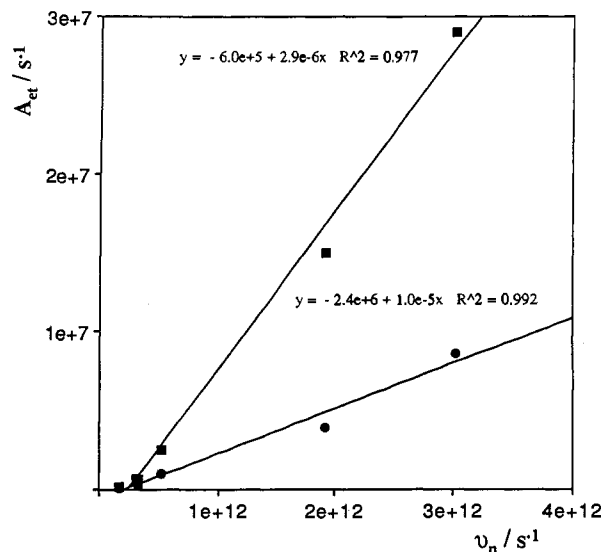


Figure 12. Dependence of the experimental pre-exponential factor, A_{et} , on the nuclear frequency factor (eq 7). The p2p monolayer data are on the top, while the p3p monolayer data are on the bottom.

hypersurface during the transition from reactants to products. By contrast, in a nonadiabatic reaction the system remains on the reactant's potential energy surface while passing through the transition state.³⁸ Since $\kappa_{el} \approx 1$ for an adiabatic reaction while $\kappa_{el} \ll 1$ for a nonadiabatic reaction, an important objective is the evaluation of the electronic transmission coefficient. This can be calculated from the preexponential factor once the nuclear frequency factor is known.³⁹

The dielectric continuum theory predicts that the nuclear frequency factor is⁴⁰

$$\nu_n = \tau_l^{-1} (\Delta\bar{G}_c^* / 4\pi k_B T)^{1/2} \quad (7)$$

Equation 7 predicts the experimentally observed negative unity slope for a plot of $\ln A_{et}$ vs $\ln \tau_l^{-1}$ (Figure 11) as long as $\Delta\bar{G}_c^*$ is independent of solvent dynamics. Figure 12 illustrates a plot of A_{et} vs the nuclear frequency factor for both monolayers. The

(37) (a) Hupp, J. T.; Dong, Y.; Blackburn, R. L.; Lu, H. *J. Phys. Chem.* **1993**, *97*, 3278. (b) Blackburn, R. L.; Hupp, J. T. *Chem. Phys. Lett.* **1988**, *150*, 399. (c) Blackburn, R. L.; Hupp, J. T. *J. Phys. Chem.* **1990**, *94*, 1790.

(38) Morgan, J. D.; Wolynes, P. G. *J. Phys. Chem.* **1987**, *91*, 874.

(39) Hupp, J. T.; Weaver, M. J. *J. Electroanal. Chem.* **1983**, *145*, 43.

(40) Zusman, L. D. *J. Chem. Phys.* **1980**, *49*, 295.

slopes of the best fit lines represent the electronic transmission coefficients. The values of κ_{el} obtained for the p2p and p3p monolayers are both considerably less than unity, indicating a low probability of electron transfer once the nuclear transition state has been attained, and therefore suggesting a nonadiabatic reaction.⁸ The small κ_{el} suggests weak coupling between the metallic states of the electrode and the localized orbitals of the redox center. The distance dependency of κ_{el} is an important internal test of these conclusions since one expects greater spatial overlap of orbitals for the shorter bridging ligands. That we observe a higher electronic transmission coefficient for the p2p monolayer (1×10^{-5}) than the p3p monolayer (3×10^{-6}) is consistent with distant dependent electronic coupling.

Existing models of electron transfer do not predict our experimental observation of an apparently nonadiabatic reaction that is strongly influenced by solvent relaxation dynamics. This point may highlight a possible deficiency in the way that electrochemical rate constants are separated into prefactors and activation components in the Butler–Volmer formalism. Apart from a deficiency in current models of electron transfer, ion pairing of the type discussed previously may be the cause of the paradox. Despite the experimental evidence in favor of an ion-pairing equilibrium that develops after electron transfer, it is conceivable that changes in ion association must precede the redox reaction. This would mean that the pre-exponential factor might include a preequilibrium constant describing the statistical probability of finding a redox center–counterion pair in a suitable configuration for electron transfer. Since ion pairing will be sensitive to the solvent properties, this pre-equilibrium mechanism could cause the overall redox kinetics to depend on the solvent, without the electron transfer event *per se* being sensitive to the relaxation rate of the solvent. However, in the preceding paper⁴ we showed that the interfacial kinetics were approximately independent of the supporting electrolyte concentration, which does not support an ion-pairing pre-equilibrium reaction. Moreover, a pre-equilibrium is more likely to produce a dependence of k on static solvent properties than on dynamic characteristics such as τ_f . We also point out that k° correlates linearly with τ_f^{-1} in a range of solvents that have different tendencies to form ion pairs.

Conclusions

Short time scale potential step methods at microelectrodes, modified with spontaneously adsorbed monolayers, alleviate many of the difficulties traditionally associated with the examination of solvent dynamic effects, including partial rate control due to diffusional transport. Complications due to mass transport are difficult to decouple from the responses observed for solution species, since diffusion rates are typically proportional to solvent viscosity, which often correlates with solvent dielectric and relaxation properties. Furthermore, the low currents observed at microelectrodes allow measurements to be made in low conductance media due to reduced iR drop. Studies of interfacial electron transfer at homogeneous monolayers also have the advantages of avoiding uncertainties regarding work terms,

stability constants, and perhaps geometries of precursor complex formation.

Our investigations suggest several deficiencies in the Butler–Volmer formulation of electrode kinetics. In particular, the experimental electrochemical enthalpy is considerably less sensitive to potential than expected. We have shown that at best only a small part of this effect is explained by a temperature-dependent transfer coefficient. In fact, our results demonstrate that this response is caused by a potential-dependent pre-exponential factor. In contrast to the problems associated with using the Butler–Volmer approach to interpret our experimental activation parameters, a model based on tunneling between electronic manifolds on the two sides of the interface qualitatively predicts many of our experimental observations.

Determination of the temperature dependence of the rate constant and formal potential has allowed us to evaluate the electrochemical free energy as a function of the solvent. The free energies evaluated from the cathodic ideal electrochemical enthalpy and the cyclic voltammetric reaction entropy agree well with those predicted for solvent reorganization by the Marcus theory. We have used these free energies of activation to determine the electronic transmission coefficient κ_{el} from the experimental preexponential factor. The electronic transmission coefficient is considerably less than unity, suggesting that the electron transfer reaction is nonadiabatic. The experimental observation that κ_{el} increases as the electron transfer distance is reduced is consistent with a reaction rate that is influenced by the extent of spatial orbital overlap between the electrode and the redox center.

However, the striking suggestion of this work is that the electrode kinetics depend strongly on solvent dynamics despite the apparently nonadiabatic character of the reaction. The implication that a nonadiabatic reaction can be heavily influenced by solvent dynamics is unexpected from contemporary theory. For the monolayers discussed here, the low electronic transmission coefficient indicates that electron transfer occurs only once out of every one hundred thousand times the transition state is formed. Under these circumstances, theory suggests that the dynamics of solvent motion would average out, leading to electrode kinetics that are independent of the relaxation rate of the solvent. However, the bare facts from this study of a family of well-behaved monolayers are that interfacial electron transfer rates are clearly linked to solvent dynamics and are also rather slow. We are not in a position to resolve this surprise, but we expect that future studies using self-organized monolayers will be essential to advancing the major objective of developing a unified understanding of the factors that influence the kinetics of interfacial electrochemical processes.

Acknowledgment. We gratefully acknowledge the financial support of the National Science Foundation under Grant CHE-86-07984 and the Defense Advanced Research Projects Agency (via the office of Naval Research and subcontract from the Massachusetts Institute of Technology) under Grant GC-R-227288.